GEOPHYSICAL RESEARCH LETTERS, VOL. 24, NO. 15, PAGES 1887-1890, AUGUST 1, 1997

Transformation shear instability and the seismogenic zone for deep earthquakes

Chris Marone and Ming Liu[1]

Department of Earth, Atmospheric, and Planetary Sciences, Massachusetts Institute of Technology, Cambridge

Abstract. We use a numerical model for olivine-spinel transformation to study deep earthquake nucleation and to delineate the seismogenic region within a subducting slab. The model includes laboratory-derived flow laws, latent heat release, and phase transformation kinetics. We calculate deformation, transformation state, grain growth, and rheology for several paths within a subducting slab. Strain rate perturbations are imposed to define the necessary conditions for instability. Strain rate perturbations decay for $\xi <$ a critical value ξ_c, and thus the coldest, interior portion of the metastable wedge deforms stably. For $\xi \geq \xi_c$, strain rate perturbations grow, shear strength decreases with strain, and the system is potentially unstable. The instability condition is mapped to delineate the seismogenic zone within a subducting slab. The model seismogenic zone is bounded by ξ_c, and, at larger percent transformations, by coarsening of spinel grains and saturation of the transformation weakening effect. The model predicts a narrow seismogenic region along the outer edges of the metastable wedge and thus a "double seismic" zone, consistent with some seismic observations. Several simplifying assumptions are required due to lack of thermo-kinetic data and incomplete knowledge of constituent mineralogy and rheology. However, the model provides a quantitative definition of the instability condition and a framework for testing the hypothesis of transformation-induced instability.

Introduction

A central problem in understanding deep focus earthquakes (> 300 km) is that of how elastically-radiated energy in the form of seismic waves can be released within a region undergoing ductile deformation. Several mechanisms have been proposed [*Frohlich*, 1989] including shear instability associated with transformation of metastable olivine to spinel [see reviews by *Green and Houston*, 1995 and *Kirby et al.*, 1996]. This hypothesis is supported by laboratory data showing instability in model materials undergoing reconstructive phase transformations and by high-resolution seismic data, which indicate that deep earthquake foci are consistent with plausible regions of olivine metastability [*Green and Burnley*, 1989; *Kirby et al.*, 1991; *Wiens et al.*, 1993; but see also *Silver et al.*, 1995]. However, existing formulations of the hypothesis lack a quantitative description of instability. Transformation weakening is not described in the context of a constitutive law that can be coupled to its surroundings to produce quantitative predictions of instability of the type necessary to test the transformational faulting hypothesis.

In contrast, for shallow earthquakes, a quantitative theory for nucleation and instability has been developed using laboratory-derived friction laws [e.g., *Roy and Marone*, 1996]. In these studies, simplified constitutive laws are combined with elastic coupling to determine the conditions for instability and parameter ranges consistent with earthquake nucleation. A similar approach may be useful in evaluating the mechanism of deep earthquakes.

In this paper, we focus on the instability condition during nucleation of deep earthquakes. We study only the onset of instability and do not consider the more general problem of rupture propagation and arrest. We use a model for coupled olivine-spinel transformation and deformation described by *Liu* [1997] who presented details of the model and showed how nucleation of deep earthquakes could be understood in terms of stability criteria. Here, we apply the model to a subducting slab and delineate the seismogenic zone for deep earthquake nucleation. We find that the system changes from stable to potentially unstable behavior with increasing transformation and thus a critical transformation for earthquake-like instability is defined.

Model and Results

We use the model of *Liu* [1997], who studied the problem of combined deformation and phase transformation in an idealized aggregate. Here, we summarize only key features of the approach and assumptions. Local regions within a subducting slab (Figure 1) are modeled as assemblages of spinel inclusions homogeneously dispersed in an olivine matrix. Interactions between inclusions and geometric effects leading to shear localization are not included. The transformation rate and latent heat release are calculated assuming grain-boundary nucleation and interface-controlled growth [e.g., *Rubie and Ross*, 1994]. Kinetic parameters are taken to be constant, independent of deformation. Creep strain and strain rate are calculated using the Eshelby-Mori-Tanaka (EMT) theory, and stress redistribution with progressive transformation is accounted for [*Liu*, 1997]. EMT theory provides a method of relating transformational strain and stress concentration, in a mean-field sense, to further deformation within the olivine framework. A key assumption we make is that volumetric transformation strain (-8%) is preserved as viscoelastic distortion in a given time step, which are kept small to account for changes in olivine-spinel abundance. The effective viscosities of olivine and spinel are constrained by flow laws of low-temperature plasticity [e.g., *Evans and Goetze*, 1979; *Liu and Yund*, 1995] and superplasticity [e.g., *Vaughan and Coe*, 1981], respectively. Spinel inclusions formed during deformation are assumed to be initially spherical (aspect ratio α=1) and α decreases with progressive deformation as inclusions become elongated with long axes perpendicular to the direction of maximum compression [e.g., *Green and Burnley*, 1989]. Because of the assumption about volumetric transformation strain, our model is applicable to temperatures $\leq\approx$ 800°C and spinel grain sizes $d_{sp} \leq\approx$ 10 μm. To simplify the range of parameters studied and to focus

[1]Now at RSM Electron Power Inc., Deer Park, NY

Paper number 97GL01851.
0094-8534/97/97GL-01851$05.00

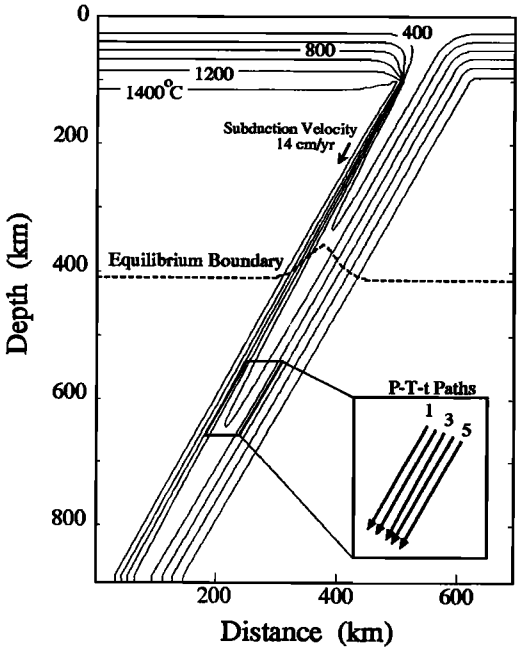

Figure 1. Thermal structure of the Tonga slab [provided by S. Stein, *Kirby et al.*, 1996]. Slab dip is 60° and the convergence rate is 14 cm/yr. This model forms the starting point for our calculations. Inset shows five pressure-temperature-time (*P-T-t*) paths along which we calculate creep deformation and transformation. Path 3 is in the coldest, central portion of the slab. The slab-perpendicular distance between adjacent paths is 7.5 km.

attention on the instability condition, we assume constant olivine and spinel grain sizes of 5 mm and 1 μm, respectively, and a constant differential stress (σ_{diff} =0.5 GPa) boundary condition. The assumption of small spinel grains is supported by numerical simulations, which indicate fine-grained spinel for low temperature transformation [*Riedel and Karato*, 1996].

Figure 1 shows slab geometry and thermal structure for the Tonga slab [*S. Stein*, pers. comm.]. We numerically evaluate deformation and transformation state along a set of pressure-temperature-time (*P-T-t*) paths parallel to slab dip (see inset to Figure 1). For each *P-T-t* path, we calculate percent transformation ξ and strain at each depth and time (Figure 2), accounting for latent heat release and adiabatic warming.

Warmer *P-T-t* paths result in greater transformation at a given depth (Figure 2a). The effect of asymmetry in the slab's thermal structure is apparent for paths just above and just below our central, coldest path (compare paths 2 and 4). For each path, the maximum shear strain increases as a function of depth and temperature (Figure 2b). Strain increases rapidly at depths ranging from 425 to 650 km. To illustrate the increase in strain rate with transformation state, we show γ versus ξ for path 3 (Figure 2c). Slab deformation increases dramatically for $\xi > 2$-3%. The strain rate for each path increases rapidly within a narrow depth interval (Figure 2d), corresponding to the increase in deformation seen in Figure 2b. With continued subduction, a second inflection in $\dot{\varepsilon}_1$ vs. depth occurs as the transformation weakening effect saturates at higher spinel abundance. We limit calculations to $d_{sp} \leq 10$ μm since above this size olivine's effective viscosity becomes lower than spinel's after only a few percent transformation, invalidating our assumption of preserved transformation strain [*Liu*, 1997].

Transformation Weakening and Shear Instability

The numerical simulations indicate that regions within the slab undergo sudden weakening and thus the possibility exists for earthquake-like instability. To analyze such a shear instability we use a generalized flow law [*Hobbs and Ord*, 1988; *Liu*, 1997]:

$$\tau = \tau(\gamma, \dot{\gamma}, \xi, \bar{\alpha}, \varepsilon^*_{ij}, d_{sp}, P, T), \qquad (1)$$

where τ is the shear stress, $\bar{\alpha}$ is the average aspect ratio of all inclusions, ε_{ij} is the average misfit strain for spinel inclusions and the other symbols have been defined above.

In this study, motivated by similar stability analyses applied to shallow earthquakes, we consider only perturbations in strain rate. We assume homogeneous axial compression and consider the instantaneous response following a perturbation. Because the corresponding time interval is small compared with other time scales in the problem (e.g. the subduction rate, the olivine-spinel transformation rate, or the spinel grain coarsening rate), ξ, d_{sp} and P are constant. In addition, we assume homogeneous deformation until a shear instability occurs, so $d\dot{\gamma}/d\gamma = 0$. After these simplifications, equations (1) can be differentiated to yield

$$\frac{d\tau}{d\gamma} = \frac{\partial\tau}{\partial\gamma} + \frac{\partial\tau}{\partial\bar{\alpha}}\frac{d\bar{\alpha}}{d\gamma} + \frac{\partial\tau}{\partial\varepsilon^*_{11}}\frac{d\varepsilon^*_{11}}{d\gamma} + \frac{\partial\tau}{\partial T}\frac{dT}{d\gamma}. \qquad (2)$$

From equation (2), if shear strength decreases with deformation upon a strain rate increase, $d\tau/d\gamma < 0$ and an instability may develop. Thus, the task of determining the necessary condition for instability consists of evaluating the sign of the terms in equation (2). The first term, $\partial\tau/\partial\gamma$, is positive since it represents strain hardening, which is accounted for by a Maxwell-viscoelastic effect in our model [*Liu*, 1997]. For the second term, spinel inclusions become more elongated with deformation [e.g., *Green and Burnley*, 1989], hence $d\bar{\alpha}/d\gamma$ is negative, and be-

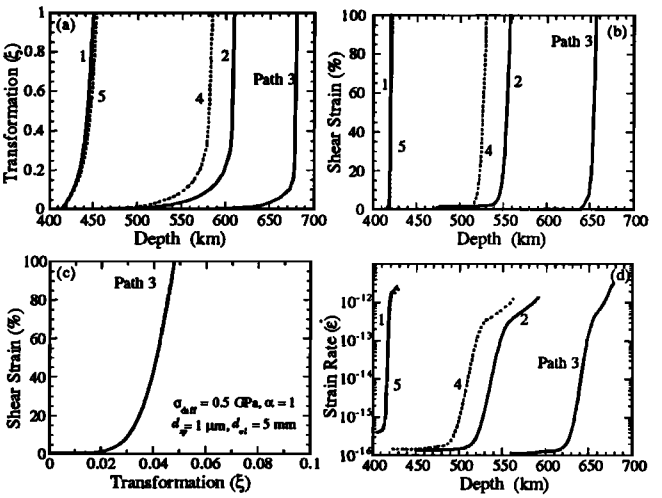

Figure 2. Numerical results for five *P-T-t* paths within the subducting slab. (a) Spinel abundance for each path, showing greater transformation for warmer paths. (b) Maximum shear strain along each path indicating a sharp onset of deformation with transformation. The large strains are an artifact of the stopping point for the calculation and our assumption of constant stress boundary conditions. (c) Details of path 3, showing rapid increase in deformation for spinel abundances of 2-3%. (d) Uniaxial strain rate for each path. Calculations extend to the depth at which spinel grains would grow to 10 μm.

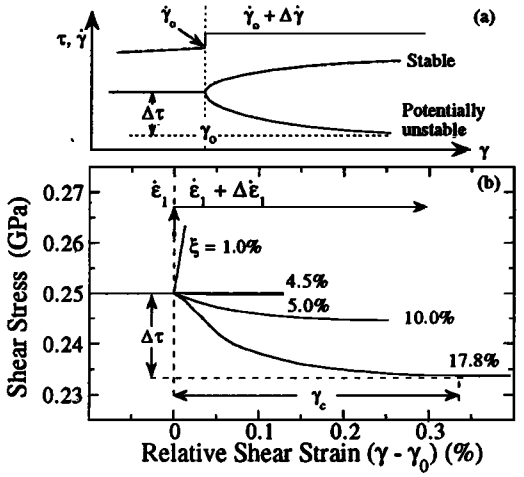

Figure 3. (a) Sketches of possible responses to strain rate perturbations. For strain $\gamma < \gamma_o$ strain rate increases slowly due to progressive creep deformation and transformation. At $\gamma = \gamma_o$, we increase strain rate at constant ξ. If strength increases the system is inherently stable. Weakening indicates potentially unstable behavior. (after *Hobbs and Ord*, 1988) (b) Calculated maximum shear strength for strain rate perturbations at five transformation states along *P-T-t* path 3. The material strengthens for low transformation (ξ<4.8%) but weakens for larger spinel abundances. The stress drop $\Delta\tau$ increases with increasing transformation.

cause the aggregate becomes stronger as spinel inclusions elongate [*Liu*, 1997], $\partial\tau/\partial\overline{\alpha}$ is also negative. Thus the second term is positive. Spinel inclusions are also weakened by more negative values of volumetric phase transformation strain, thus $\partial\tau/\partial\varepsilon_{11}^{*}$ is positive. $d\varepsilon_{11}^{*}/d\gamma$ is either positive or negative depending on the relative flow rate of the matrix and inclusions. For geological materials $dT/d\gamma$ and $\partial\tau/\partial T$ are positive and negative respectively and thus shear heating yields weakening [e.g., *Hobbs and Ord*, 1988]. Thus the last two terms in equation (2) could lead to instability. However, for strain rates relevant to the onset of instability (e.g., Figure 2d), shear heating is not expected to be significant. That is, we focus on the initial onset of instability during earthquake-like nucleation. Once shear accelerates and higher strain rates are attained, shear heating may be important. Also, although latent heat release may be critical for producing the conditions necessary for instability [e.g., *Green and Zhou*, 1996], *Liu* [1997] showed that nucleation of the olivine-spinel transformation instability occurs even without latent heat (although he emphasized the importance of latent heat for quasistatic yielding leading to nucleation). Our model accounts for latent heat release, however, we do not consider possible variations in transformation kinetics [e.g., *Kerschhofer et al.*, 1996].

From this analysis, transformation weakening and instability depend on the third term in equation 2. We calculate this effect as a function of transformation state and strain by imposing strain rate perturbations (Figure 3). To perform the perturbations we change from a stress boundary condition, for $\gamma < \gamma_o$, to a strain rate boundary condition at fixed transformation state. Figure 3a shows hypothetical responses. Strengthening results in stable behavior, whereas weakening is potentially unstable. Figure 3b shows calculated responses to a series of perturbations, imposed as step changes in uniaxial strain rate. The magnitude of the perturbations are 5% of the strain rate at $\gamma=\gamma_o$. For spinel abundance less than a critical value ξ_c, strengthening occurs and the system is stable. However, for $\xi > \xi_c$, the material weakens with shear. For the parameters of Figure 3b, ξ_c is 4.8%. The degree of weakening increases with increasing transformation. By evaluating a series of paths we find that ξ_c is weakly dependent on *P-T-t* path, varying from 1-5% from the warmest to coldest path.

The Seismogenic Zone for Deep Earthquakes

In Figure 4, we combine results from strain rate perturbations along each *P-T-t* path to map the seismogenic zone within the subducting slab. In the cold interior of the metastable wedge, spinel transformation is kinetically inhibited. In the region $0 < \xi < \xi_c$ strain rate perturbations indicate stable deformation (Figure 4a). The seismogenic zone is defined between ξ_c and the upper limit of spinel grain size d_{sp} for transformation weakening, which we take as 10 μm [*Liu*, 1997]. By the time spinel grains coarsen to 10 μm, the phase transformation strain is effectively zero and thus differential stress in the inclusions is too small to continue driving the transformation weakening effect, even if spinel were weaker than olivine [*Liu*, 1997]. The resulting seismogenic zone is a narrow region along the outer edge of the metastable wedge, with the outer limit at 10-18% transformation (Figure 4a).

Discussion

Our calculations indicate that nucleation of deep earthquakes by the transformational faulting mechanism is confined to a narrow region along the edge of the metastable wedge. For the subduction zone considered, the model predicts a double seismic zone, consistent with observations from Tonga and Izu-Bonin [e.g., *Wiens et al.*, 1993]. The possible significance of this is un-

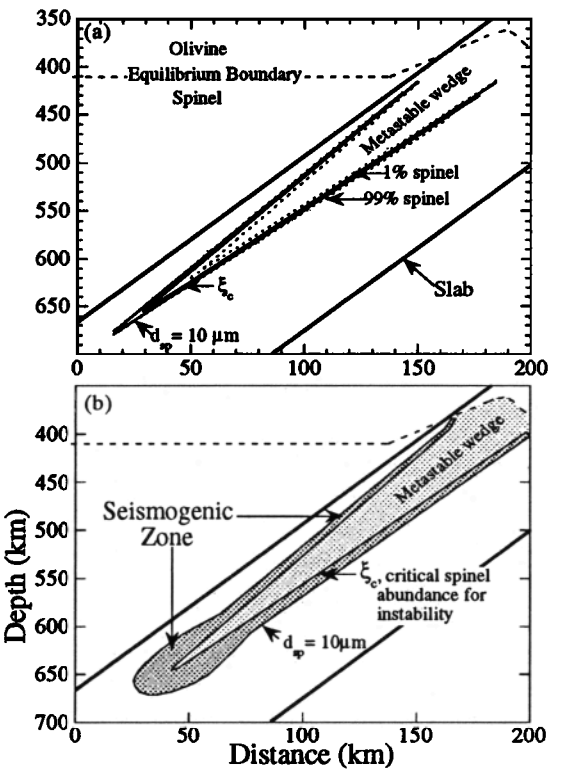

Figure 4. Seismogenic zone within the slab and metastable wedge. (a) Dashed lines show beginning and end of olivine-spinel transformation. Solid lines show boundaries of the seismogenic nucleation region, as defined by the critical transformation for weakening ξ_c and the point at which the transformation weakening effect ceases due to spinel coarsening. (b) Cartoon showing broadening of the seismogenic zone with depth due to internal slab deformation and inhomogeneities in the boundary between partial and complete transformation.

clear given that we consider only one subduction zone and thermal model and since observed differences in focal mechanisms for the upper and lower zones in Tonga are not explained in the context of our model. Also, limitations of the constitutive model and uncertainties associated with thermo-kinetic parameters make boundary positions somewhat uncertain. Nevertheless, the existence of an inner boundary of the seismogenic zone defined by ξ_c and the limited extent of the seismogenic region within the metastable wedge are generic features and would persist for a wide range of slab thermal states and constitutive parameters.

The narrowness of the predicted seismogenic region appears to contradict observations from recent deep earthquakes [e.g., *Silver et al.*, 1995; *Stein*, 1995.]. Estimated source dimensions and aftershock distributions of these events exceed estimates of the metastable wedge width (although we note that such estimates are also subject to uncertainties in thermo-kinetic parameters). However, our calculations only address nucleation of instability for small strain rates within an initially-homogeneous material. Shear heating and other factors are likely to be important during dynamic rupture propagation. In this case, rupture propagation out of the seismogenic zone is not unexpected. Moment release in such regions requires only access to stored elastic energy and the existence of a region of conditional stability. This does not pose a serious problem for propagation within the metastable wedge, but as pointed out by *Silver et al.*, [1995] large propagation distances within a fully transformed region may require additional mechanisms. *Silver et al.* [1995] suggest reactivation of preserved zones of weakness to explain large source dimensions, however, this does not address rupture nucleation. The main problem in estimating the potential propagation distance out of the metastable wedge appears to be access to stored elastic energy, since several factors may smear the boundary between partially- and fully-transformed material. Such factors include compositional heterogeneity, preserved zones of weakness, heterogeneities due to variations in thermal and transport properties, and broadening of the transforming zone via deformation.

Figure 4b shows a cartoon of a broadened zone of transformation with increasing depth. Such broadening is suggested by the narrow depth interval of deformation (Figure 2b), which for fast subduction velocity implies nearly adiabatic deformation (excepting the latent heat release). This is equivalent to broadening the isotherms without significantly reducing the region of metastable olivine [e.g., *Stein*, 1995]. This supports previous suggestions of slab thickening [cf. *Green and Houston*, 1995; *Kirby et al.* 1996; *Karato*, 1997] and is consistent with seismic tomographic studies indicating slab thickening and distortion in the transition zone [e.g., *van der Hilst*, 1995]. However, buoyancy considerations limit thickening of the metastable wedge and it is important to quantitatively assess such thickening in a model that integrates thermal effects with slab stresses and deformation.

Conclusions

We use a model for coupled transformation and deformation to study the onset of shear instability and delineate the seismogenic zone in a subducting slab. The model represents a first attempt to construct a realistic constitutive law that can be coupled with a description of continuum interactions for quantitative study of deep earthquake nucleation. We find a transition from stable to potentially unstable behavior above a critical spinel abundance ξ_c. Our model seismogenic zone is bounded by ξ_c and a maximum spinel grain size and consists of a narrow region at the outer edge of the metastable wedge. A zone of conditional stability is expected to surround this region, such that rupture may propagate outside the nucleation region or be triggered there by sufficiently large perturbations. Several simplifying assumptions are required due to lack of thermo-kinetic data and incomplete knowledge of constituent mineralogy and rheology and these should be addressed in future models.

Acknowledgments. We thank S. Stein for the Tonga thermal model and C. Frolich, S. Karato, D. Rubie, and S. Stein for critical comments on the manuscript. We also thank for H. Green, G. Schubert, and H. Houston for stimulating discussions on this topic. This work was supported by an NSF Postdoctoral fellowship to ML (EAR-9404244) and by NSF grants EAR-9316082 and EAR-9629472 to CM.

References

Evans, B. and C. Goetze, The temperature variation of hardness of olivine and its implications for polycrystalline yield stress, *J. Geophys. Res.*, *84*, 5505-5524, 1979.

Frohlich, C., The nature of deep-focus earthquakes, *Ann. Rev. Earth Planet. Sci.*, *17*, 227-254, 1989.

Green, H. W., and P. C. Burnley, A new self-organizing mechanism for deep-focus earthquakes, *Nature*, *341*, 733-737, 1989.

Green, H. W. and H. Houston, The mechanics of deep earthquakes, *Ann. Rev. Earth Planet. Sci.*, *23*, 169-213, 1995.

Green, H. W. and Y. Zhou, Transformation-induced faulting requires an exothermic reaction and explains the cessation of earthquakes at the base of the mantle transition zone, *Tectonophys. 256*, 39-56, 1996.

Hobbs, B. E., and A. Ord, Plastic instabilities: implications for the origin of intermediate and deep focus earthquakes, *J. Geophys. Res.*, *93*, 10521-10540, 1988.

Karato, S. Phase transformation and rheological properties of mantle minerals, in Earth's Deep Interior, ed. D. Crossley and A. M. Soward, Gordon and Breach Sci. Publ., p. 223-272, 1997.

Kirby, S. H., W. B. Durham, and L. A. Stern, Mantle phase changes and deep-earthquake faulting in subducting lithosphere, *Science*, *252*, 216-225, 1991.

Kirby, S. H., S. Stein, E. Okal, and D. C. Rubie, Metastable mantle phase transformations and deep eqs, *Rev. Geophys.*, *34*, 261-306, 1996.

Kerschhofer, L., T. G. Sharp, and D. C. Rubie, Intracrystalline transformation of olivine to wadsleyite and ringwoodite under subduction zone conditions, *Science*, *274*, 79-81, 1996.

Liu, M., A constitutive model for olivine-spinel aggregates and its application to deep earthquake nucleation, *J. Geophys. Res.*, *102*, 5295-5312, 1997.

Liu, M., and R. A. Yund, The elastic strain energy associated with the olivine-spinel transformation and its implications, *Phys. Earth Planet. Int.*, *89*, 177-197, 1995.

Riedel, M. R., and S. Karato, Microstructural development during nucleation and growth, *Geophys. J. int.*, *125*, 397-414, 1996.

Roy, M. and C. Marone, Earthquake nucleation on models faults with rate and state dependent friction: the effects of inertia, *J. Geophys. Res.*, *101*, 13,919-13,932, 1996.

Rubie, D. C., and C. R. Ross II, Kinetics of the olivine-spinel transformation in subducting lithosphere: exp. constraints and implications for deep slab processes, *Phys. Earth Planet. Int.*, *86*, 223-241, 1994.

Silver, P. G., S. L. Beck, T. C. Wallace, C. Meade, S. C. Myers, D. E. James, and R. Kuehnel, Rupture characteristics of the deep Bolivian earthquake of 9 June 1994 and the mechanism of deep-focus earthquakes, *Nature*, *268*, 69-73, 1995.

Stein, S., Deep earthquakes: A fault too big?, *Science*, *268*, 49-50, 1995.

van der Hilst, R., Complex morphology of subducted lithosphere in the mantle beneath the Tonga trench, *Nature*, *374*, 154-157, 1995.

Vaughan, P. J., and R. S. Coe, Creep mechanism in Mg2GeO4: effects of a phase transition, *J. Geophys. Res.*, *86*, 389-404, 1981.

Wiens, D. A., J. J. McGuire, and P. J. Shore, Evidence for transformational faulting from a deep double seismic zone in Tonga, *Nature*, *364*, 790-793, 1993.

M. Liu and C. Marone, Dept. of Earth, Atmospheric, and Planetary Sciences, MIT, Cambridge, MA 02139 (email: cjm@westerly.mit.edu)

(Received April 15, 1997; Accepted June 13, 1997.)